Photodesorption and Trapping of Molecular Oxygen at the TiO_2(110)−Water Ice Interface†

Craig L. Perkins‡ and Michael A. Henderson*

Environmental Molecular Sciences Laboratory, Pacific Northwest National Laboratory, P.O. Box 999, MS K8-93, Richland, Washington 99352

Received: September 5, 2000

By means of temperature programmed desorption (TPD), static secondary ion mass spectroscopy (SSIMS), and electron energy loss spectroscopy (EELS), we have investigated further the states of oxygen adsorbed on rutile TiO_2. Previous work has shown that annealing the (110) surface in a vacuum produces isolated bridging oxygen vacancies, and that these vacancies are intimately connected with molecular and dissociative oxygen adsorption channels. We find that at 115 K illumination of the oxygen-exposed surface with 4.1 eV photons results in photodesorption of the oxygen associated with a TPD state centered on 410 K, in contrast to the remaining oxygen destined for a dissociative channel. An unusual effect of water overlayers on the photochemical properties of the O/TiO_2(110) system is explored. For thick overlayers, it is possible to generate via UV irradiation a previously unobserved oxygen TPD state. Evidence is presented for this new O_2 TPD state originating from the photolysis of an O_2−water adduct.

I. Introduction

The ternary system consisting of molecular oxygen, water, and a metal oxide is a prominent player in photocatalysis, astrophysics, and atmospheric studies. TiO_2 in particular has served as a model photocatalyst.[1] It was found some time ago that TiO_2-coated surfaces could be made photoactive enough to catalytically oxidize hydrocarbons accumulated from the atmosphere.[2] Additionally, the sanitary conditions required in hospitals and breweries can be partially achieved by the biocidal properties of photoactive TiO_2.[2] The powerful lure of self-cleaning windows, optical components, and environmentally benign wastewater treatment has resulted in a steady stream of papers demonstrating that, under certain conditions, the rutile and anatase polymorphs of TiO_2 can function as efficient and selective photooxidation catalysts. In all of these uses, the interplay among molecular oxygen, water, and light are important to the photooxidation processes occurring on TiO_2.

Similar photochemical processes occur, and possibly on a much greater scale, in our own atmosphere where oxygen, water, and metal oxide aerosols are in constant contact with organic species. In a similar sense, oxygen−ice−oxide mixtures are most likely to be present in water-bearing lunar and Martian soils which have been exposed to light. In places such as the surface of Ganymede where oxygen, water, and dust mixtures coexist,[3,4] it is not inconceivable that photocatalytic processes occurring on solid surfaces might have a significant influence on atmospheric composition since most solid oxide materials have much larger absorptivities for solar radiation than typical low molecular weight atmospheric constituents. In diffuse, translucent molecular clouds, photocatalytic processes on the surfaces of interstellar grains of oxides and graphite covered with icy mantles of adsorbates are thought to play an important role in the abundances of several molecular species.[5]

Despite the prevalence and importance of the oxygen−water−metal oxide system, and the many published investigations of them, many unsettled questions still remain regarding the interactions of light with model systems exemplified by oxygen−water−rutile TiO_2(110). Debate continues over the traditional picture of photooxidation on oxide surfaces in which molecular oxygen plays an indirect role by functioning as an electron scavenger, leaving the oxidation to be performed directly by holes or by proxy through hydroxyl radicals. The initial reaction occurring upon absorption by TiO_2 of above band gap light is generation of the electron−hole pair:

$$TiO_2 \rightarrow h^+ + e^- \quad (1)$$

If recombination is avoided, both the electron (e^-) and hole (h^+) can participate in chemical reactions. Proposed reactions involving holes include the following:

$$h^+ + OH^- \rightarrow \bullet OH \quad (2)$$

$$h^+ + H_2O \rightarrow H^+ + \bullet OH \quad (3)$$

$$h^+ + RCH_2R' \rightarrow R\bullet CHR' + H^+ \quad (4)$$

$$R\bullet CHR' + \bullet OH \rightarrow RCOHR' \quad (5)$$

$$RCH_2R' + \bullet OH \rightarrow R\bullet CHR' + H_2O \quad (6)$$

In reactions 1−6 it would appear that photooxidation could take place without the participation of photogenerated electrons or oxygen, as long as there was a trap for the electrons to keep them from recombining with holes. The most common electron sink was thought to be molecular oxygen (reaction 7).

$$e^- + O_2 \rightarrow O_2^- \quad (7)$$

However, by independently suppressing the involvement of electrons (by making use of $e^- + Fe^{3+} \rightarrow Fe^{2+}$) and molecular oxygen (by excluding O_2), Heller et al. found that photooxida-

† Part of the special issue "John T. Yates, Jr., Festschrift".

* Corresponding author. E-mail: ma.henderson@pnl.gov.

‡ Permanent address: National Renewable Energy Laboratory, 1617 Cole Blvd, MS 3215, Golden, CO 80401-3393.

10.1021/jp0031799 CCC: $20.00
Published on Web 03/13/2001

tion of a series of aliphatic hydrocarbons, alcohols, ketones, carboxylic acids, and aldehydes did not proceed unless oxygen was present.[2] The authors' conclusion that molecular oxygen was necessary for photooxidation even in the presence of an electron scavenger such as Fe^{3+} was explained by the formation of unstable hydrotetroxides as in reactions 8−10.

$$O_2^- + H^+ \rightarrow \bullet OOH \quad (8)$$

$$R\bullet CHR' + O_2 \rightarrow RCH(\bullet OO)R' \quad (9)$$

$$RCH(\bullet OO)R' + \bullet OOH \rightarrow RCH(OOOOH)R' \rightarrow RCOR' + O_2 + H_2O \quad (10)$$

Additionally, Muggli and Falconer found evidence for an active oxygen intermediate which exchanged oxygen with water adsorbed in powdered TiO_2 photocatalysts.[6] Gu et al. showed that photooxidation of CH_3Cl on TiO_2(110) involved activated molecular oxygen rather than hydroxy radicals.[7] Evidence has been found for a photogenerated chemical species that is capable of entering the gas phase and remotely performing oxidative chemistry.[8] In these latter experiments the authors found that the presence of molecular oxygen promoted strongly the remote bleaching effect.

No such direct role for O_2 has yet been established in more fundamental studies on single-crystal TiO_2 photocatalysts. In previous work we have examined the fundamental properties of oxygen[9,19] and water[11] on the well-defined single-crystal rutile TiO_2(110). In brief, at low temperatures on the nearly perfect (110) surface the first monolayer of water prefers to adsorb molecularly at five-coordinate Ti^{4+} and yields in TPD experiments a peak centered on ∼270 K and loss features in HREELS at 3420−3505 and 1605 cm^{-1}. At higher water coverages a second TPD state is seen at 174 K. Loss features below 3300 cm^{-1} were used to assign this water state to second layer water that is hydrogen bonded to anion sites. TPD and HREELS spectra show the formation of an ice multilayer at coverages above 2 monolayers (ML; 1 ML = $5.2 \times 10^{14}/cm^2$). The stoichiometric (110) surface was found to not adsorb molecular oxygen at temperatures greater than 100 K.

The chemistry of oxygen and water on the vacuum annealed surface was substantially different than on the nearly perfect surface. Rutile samples were prepared by annealing at >850 K until the samples were light blue to the eye, and were initially cleaned of the major impurities (Na, K, Al, Ca) by sputtering with 2−3 keV Ar^+. Subsequent cleaning cycles consisted of gentle (500 eV) argon ion sputtering followed by 10 min UHV anneals at 850 K. Prepared under these conditions, the surface yields high quality $p(1 \times 1)$ LEED patterns and is slightly oxygen deficient. Oxygen vacancies consist primarily of missing two-coordinate bridging anions and locally reduced Ti^{3+} sites. Water absorption on this surface results in dissociation at bridging oxygen vacancies with the production of bridging hydroxyl groups.[11−13] These bridging hydroxyl groups provide a simple sensitive way to quantify anion vacancies because the hydroxyls recombinatively desorb in a distinct TPD state centered on 500 K.

On the vacuum annealed surface molecular oxygen was found to display complicated precursor state driven adsorption and desorption kinetics. King and Wells type oxygen uptake experiments indicated that at 120 K initial sticking coefficients were high, that three oxygen molecules were adsorbed per bridging oxygen vacancy, and that all adsorbed molecules resided in the shallow potential well of a precursor state. The structure of the low-temperature oxygen molecules was proposed to follow a model in which one O_2 (η_2) was adsorbed side-on directly over a bridging oxygen vacancy, and two adjacent O_2 molecules (η_1) were adsorbed end-on at the in-plane five-coordinate Ti^{4+} cations.[9] Heating the oxygen-dosed surface during TPD experiments showed that two-thirds of the total O_2 (all η_1 O_2) desorbed molecularly, whereas the remaining molecules dissociated and reoxidized the Ti^{3+} sites, leaving reactive oxygen atoms on the surface. These O adatoms could not be directly detected by TPD, but their presence was inferred from isotopically labeled reactions involving water.

In this study, we have reexamined the photochemistry of the oxygen/TiO_2(110) system both with and without coadsorbed water. We find strong evidence for *incomplete* removal of adsorbed oxygen by exposure of the surface to above band gap photons. Additionally, we show that the O_2 molecules destined for the molecular adsorption channel may react with water to form a photochemically active species, whereas the oxygen adsorbed directly at bridging oxygen vacancies and destined for the dissociative channel remains on the surface even with high water coverages. The photodesorption of adsorbed oxygen has been followed using postirradiation TPD, and we find that the photodesorbed oxygen observed by Yates et al.[14,15] originates from the 410 K TPD state previously observed in our laboratory.[9,10] In contrast, a new molecular oxygen TPD state at ∼140−160 K, produced by the irradiation of oxygen with water overlayers, is associated with the photolysis of a photochemically active TiO_2(110) surface species. This photoactive oxygen species trapped at the TiO_2−ice interface may be directly analogous to photoactive oxygen species believed to be formed at the heterogeneous TiO_2−solution interface.

II. Experimental Section

The experiments were performed in a stainless steel ultrahigh vacuum (UHV) chamber which has been described previously.[11] In brief, the system has a base pressure of less than 5×10^{-11} Torr and is equipped with instrumentation for high-resolution electron energy loss spectroscopy (HREELS), Auger measurements (AES), static secondary ion mass spectrometry (SSIMS), low energy electron diffraction (LEED), and temperature programmed desorption (TPD), as well as a calibrated pinhole doser and the usual facilities for sample cleaning. A 100 W Oriel Hg arc lamp (Model 68805) was used in conjunction with a water IR filter, a 4.13 ± 0.07 eV band pass filter, and (where noted) neutral density filters to irradiate the samples. To be able to directly compare TPD and photodesorption data, the crystal was positioned directly facing the mass spectrometer such that the face of the crystal could be illuminated by the image of the Hg arc. The angle between the crystal normal and UV beam was ∼50°. The photon flux from the arc lamp was calibrated with a power meter (Molectron EPM 1000) equipped with a thermopile detector (Molectron PM3). Constant power to the rutile crystal was maintained by a photodiode feedback system. Temperature increases due to lamp illumination were found to be less than 3 K.

The Hg arc lamp was designed to perform most reliably at full output power, so low photon exposures were obtained not by turning down the arc current, but rather by using a metal film neutral density filter having an optical density (OD) of 1.0. Exposure times were then corrected to the "no filter" condition. To ensure that the neutral density filter behaved as expected at the wavelengths used, exposures corresponding to Ft, where F is the flux in photons/s and t is the time in seconds, were repeated, once with the 1.0 OD filter in place using an exposure

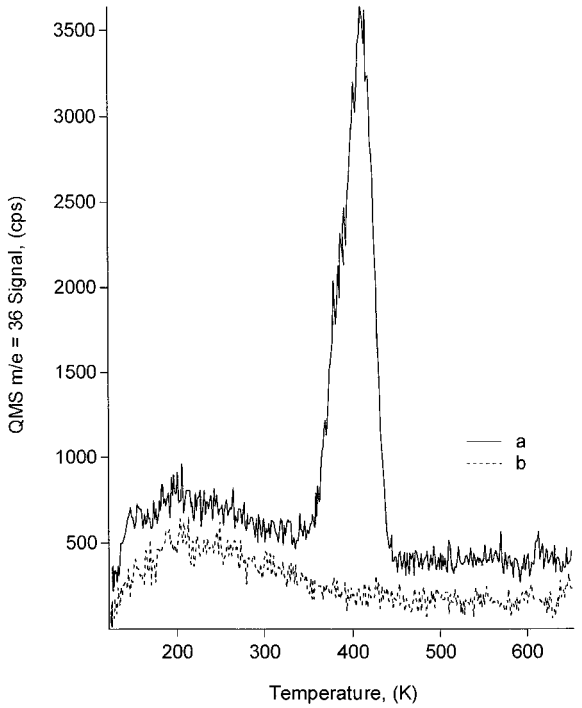

Figure 1. $^{18}O_2$ TPD spectra from TiO_2(110): (a) no light exposure; (b) exposure to 2.1×10^{17} photons/cm^2 ($h\nu = 4.13$ eV).

time of 10*t*, and once without the filter using an exposure time of *t*. No significant difference in the photodepletion of the 410 K O_2 peak was noted between the two experimental arrangements. A single crystal of Si(100) mounted in an identical fashion and opposite the rutile crystal served as a control for oxygen adsorption/photodesorption experiments. Photodesorption of oxygen was not observed from the crystals' supporting tantalum rods and wires or from the chamber walls.

The single-crystal TiO_2(110) sample (MarkeTech International Inc.) was initially cleaned by a series of argon sputtering and annealing cycles. Multiple vacuum anneals at 850 K were performed such that the crystal was conductive, had a translucent blue color, and yielded sharp $p(1 \times 1)$ LEED patterns. For the experiments discussed here, the standard cleaning procedure consisted of a 10 min anneal in UHV at 850 K followed by a quench to 115 K. A typical cooling time was on the order of 20 min. This procedure created a surface with an oxygen vacancy concentration (determined via water TPD experiments) of ~10% of 1 monolayer (ML), where 1 ML is defined in terms of the number of TiO_2(110) unit cells per square centimeter (5.1×10^{14}). Unless noted otherwise, oxygen and water exposures were done while maintaining the crystal at 115 K.

III. Results and Discussion

A. Thermal and Photodesorption from O_2-Precovered TiO_2(110). On the basis of photodesorption cross section measurements, Yates et al.[14,15] have proposed three different bonding arrangements of molecular oxygen on TiO_2(110). Their model for oxygen adsorption has one molecule per bridging oxygen vacancy, with two low-temperature photodesorption states denoted α_1 and α_2, both of which may be converted to a state labeled β by heating to between 250 and 400 K. They did not observe the molecular oxygen thermal desorption peak which we have seen at 410 K,[9,10] although this state has also been observed by Brinkley and Engel,[16] and Yanagisawa and Ota.[17] Figure 1 shows TPD data from which a connection can be made between the α photodesorption states observed by Yates et al. and the 410 K TPD state. Shown in Figure 1a is a TPD spectrum of the vacuum annealed surface dosed first with $^{18}O_2$ (4.5×10^{15} molecules/cm^2) and then, *on one portion of the crystal*, with several monolayers of $H_2{}^{16}O$, whereas in Figure 1b is a TPD spectrum of the sample prepared in the same manner but exposed to 2.1×10^{17} photons/cm^2 during the time between the oxygen and water exposures. Under dark conditions, the normal 410 K molecular oxygen peak is obtained, albeit slightly attenuated by the water adsorption. (The reason for employing water overlayers and the nature of the interaction between coadsorbed oxygen and water will be further discussed below.) When the oxygen-dosed surface is illuminated with 4.1 eV light, the 410 K TPD state is completely depleted. We can therefore conclude that the 410 K TPD state measured in this and previous studies in our group most likely stems from the same molecular oxygen species that Yates et al. have designated as α_1 and α_2.

The photodesorption of molecular oxygen from TiO_2(110) has been proposed to involve several steps: generation of the electron−hole pair, degeneration of these into free carriers, diffusion of the carriers, capture of a hole by negatively charged oxygen molecules, and finally desorption of O_2.[14,17] Although this picture of capture of a hole by an oxygen species is contrary to the usual scenario of electron capture by oxygen,[13] the physical situation of an n-type semiconductor such as TiO_2 with a depletion layer (from O_2 adsorption) dictates that holes rather than electrons are driven to the surface.[18−20] Since the driving force for this hole migration to the surface is upward band bending (resulting from the $O_{2(ad)}{}^{\delta-}$ derived depletion layer) and the band bending itself is a function of oxygen coverage, the photodesorption kinetics were predicted to be first order and to follow

$$N(t) = N_0 e^{-(FQt)}$$

where the $N(t)$ is the oxygen coverage at time t, N_0 is the initial coverage, F is the light intensity, and Q is the photodesorption cross section.[14,15,17] Using this model, we have estimated the photodesorption cross section of the molecules in the 410 K TPD state from the decrease in the TPD peak area as a function of photon exposure. The results obtained for 4.13 ± 0.07 eV light are plotted in Figure 2. The slope of the least-squares line through the 410 K O_2 TPD state depletion data in Figure 2 is equal to the product of the photon flux and the photodesorption cross section. Using the flux determined for our lamp (see section II), we calculate a cross section for the photodepletion of the 410 K O_2 TPD state of 1.9×10^{-17} cm^2, consistent with the previously published value by Yates et al.[13,14] of $(4.0 \pm 0.5) \times 10^{-17}$ cm^2 at 3.94 ± 0.07 eV for the dominant "α_2" oxygen bonding arrangement. This is additional verification that our 410 K O_2 TPD state stems from the same molecular oxygen species as the oxygen designated by Yates and co-workers as "α_2".

We have found it helpful to use the adsorption/desorption of water as a probe of the status of oxygen on the TiO_2(110) surface. Bridging oxygen vacancies produced during vacuum anneals are active sites for water dissociation,[11−13] and are therefore easily detected and quantified using water TPD. Figure 3a is a typical TPD spectrum of water from the vacuum annealed TiO_2(110) surface. For clarity, lower temperature desorption peaks from second and multilayer water are not shown. In water TPD from the vacuum annealed surface, recombinative desorption of water from bridging −OH groups occurs at ~520 K (Figure 3a), whereas the water desorbing at 270 K is from molecularly adsorbed species at five-coordinate Ti^{4+} sites.

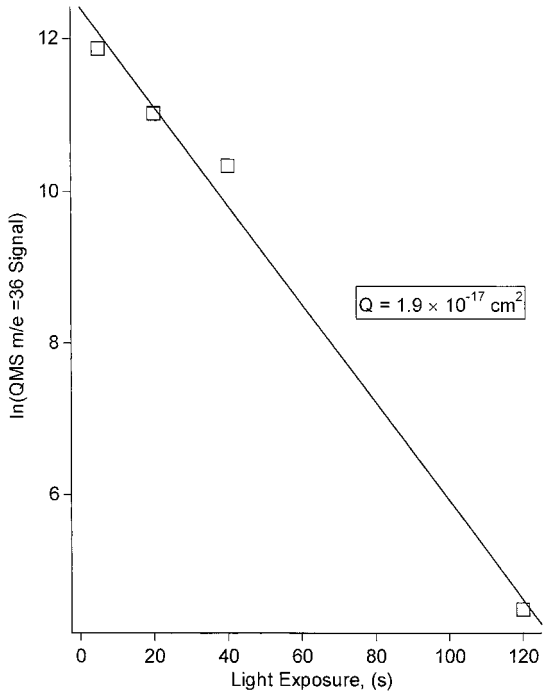

Figure 2. Depletion of the 410 K O_2 TPD state as a function of light exposure. The slope of the semilog (1.9×10^{-17}) is equal to the photodepletion cross section.

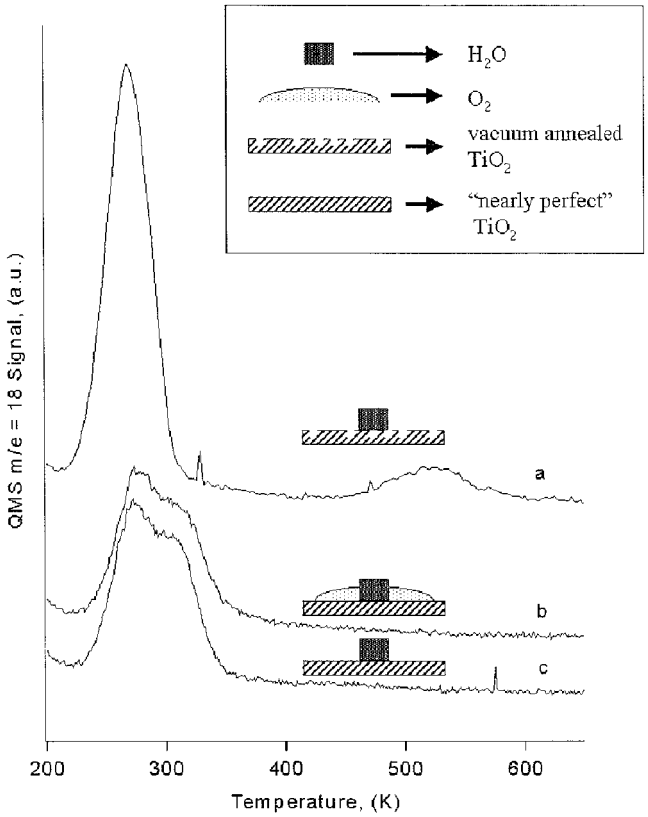

Figure 3. (a) Reference TPD spectrum of water desorption from vacuum annealed TiO_2(110). In (b) and (c) are water TPD traces from the experiments in Figure 1: (b) no light exposure; (c) exposure to 2.1×10^{17} photons/cm^2 ($h\nu = 4.13$ eV). For clarity the second layer and multilayer desorption peaks are omitted.

We have recently found that a new water TPD peak centered on ~300 K results from the presence of oxygen adatoms left over from the reaction between isolated anion vacancies and O_2 molecules.[10] In Figure 3b is the water desorption trace

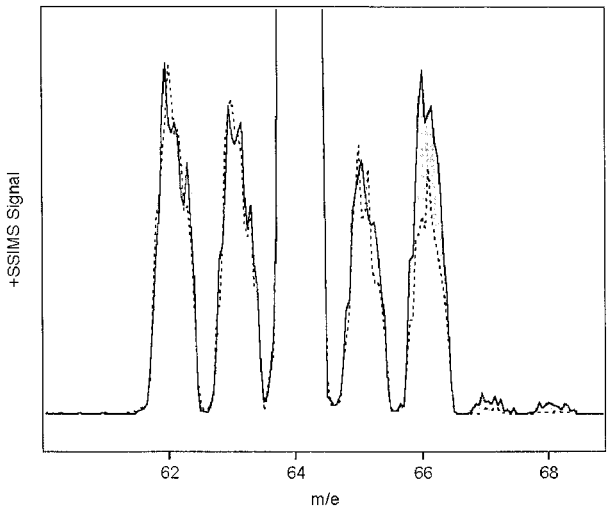

Figure 4. Static SIMS data of the clean, vacuum annealed TiO_2(110) surface (dotted line), and of the surface after a single $^{18}O_2$ adsorption/photodesorption cycle. Major differences between the two spectra are shaded gray.

obtained concurrently with the oxygen signal of Figure 1a, the experiment in which the vacuum annealed sample was dosed first with oxygen and then with water. The accompanying schematic of the system as it was before the temperature ramp of the TPD experiment is meant to show (1) qualitatively the relative sizes and position of the regions of the crystal which have been dosed with H_2O and O_2 and (2) the fact that the bridging oxygen vacancies are not present at the time of the water exposure. (The fact that H_2O and O_2 do not have identical angular divergences when emerging from our doser is important and is discussed further in section IIIB.) The 520 K water TPD state is not seen in Figure 3b because the oxygen vacancies that were generated by the vacuum anneal have been filled by the preadsorbed O_2 molecules. The shoulder on the high-temperature side of the 270 K molecular desorption peak is characteristic of the aforementioned reaction between oxygen adatoms and water molecules.[10] Figure 3c is the water TPD trace from the experiment of Figure 1b in which the vacuum annealed crystal was first dosed with oxygen, then exposed to 2.1×10^{17} photons/cm^2 ($h\nu = 4.13$ eV), and finally dosed with our probe molecule, water. The schematic of the system depicts a water layer on top of the "nearly perfect" surface (i.e., a surface in which there are almost no bridging oxygen vacancies) and depicts the photoassisted removal of the preadsorbed O_2 which is associated with the 410 K O_2 TPD state. The fact that there is not a discernible water desorption state near 520 K demonstrates that at least some of the adsorbed oxygen has remained on the surface *despite* the UV irradiation, and that it has dissociated and filled in bridging oxygen vacancies that were generated during vacuum annealing. The shoulder on the 270 K H_2O molecular state is also evidence that the UV radiation does not remove the oxygen molecules that generate oxygen adatoms via reaction with isolated O vacancies.

Further evidence for oxygen remaining behind on the TiO_2-(110) surface after a photodesorption event is provided by the SSIMS data of Figure 4. The dashed line in Figure 4 represents SSIMS data of the clean, vacuum annealed surface. The series of peaks centered on $m/e = 64$ (TiO^+) reflect the isotopic abundances of titanium since naturally occurring oxygen is comprised almost entirely of ^{16}O. The upper, solid line in Figure 4 is a SSIMS spectrum of the surface after being dosed with 5.2×10^{15} $^{18}O_2$ molecules/cm^2, and then exposed to the UV source for a period 10 times longer than was typically needed

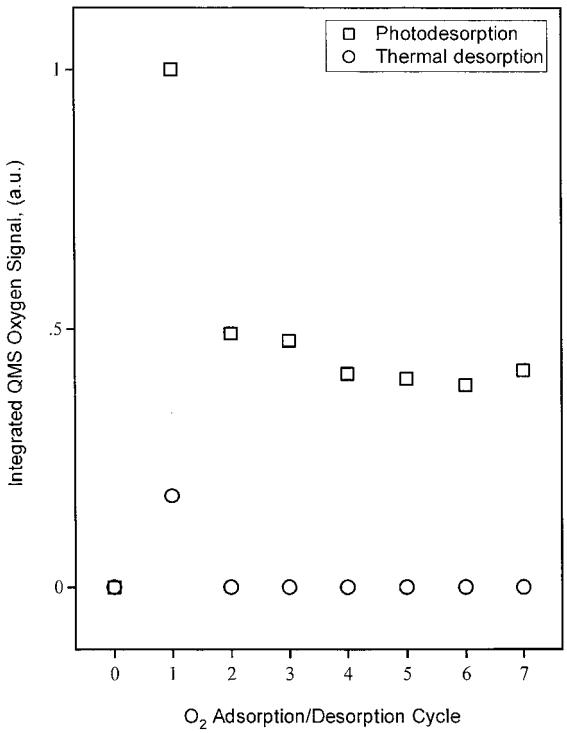

Figure 5. Plots of integrated oxygen signal obtained from a series of thermal and photodesorption experiments. Adsorption/desorption cycle 0 corresponds to thermal and photodesorbed oxygen from the vacuum annealed surface that had not been exposed to O_2 (no oxygen was detected in either case).

for the signal due to photodesorbing $^{18}O_2$ to completely decay. From the difference between the two spectra (shaded regions), it can be seen that a significant fraction of the ^{18}O initially adsorbed upon the surface has remained after extensive exposure to UV light. If we assume that the TiO^+/Ti^+ ratio (Ti^+ data not shown) approximately represents the surface oxygen concentration in the first layer of the crystal lattice, then the amount of ^{18}O remaining after the photodesorption is about 3.7% of the total surface oxygen (bridging and in-plane), or 11% of the bridging oxygen. In comparison with the amount of ^{18}O expected to be deposited onto the surface (one O_2 molecule per bridging O vacancy, or twice the 10% vacancy population as measured by water TPD), this is about half what one would expect. We attribute this discrepancy to the well-known difficulties that accompany quantification of SIMS data. Qualitatively, we can safely arrive at the important conclusion that prolonged irradiation of oxygen-adsorbed TiO_2(110) with photons having energies greater than the rutile band gap does not completely remove all of the adsorbed oxygen.

There remains a final interesting difference between thermal and photodesorption of oxygen from TiO_2(110). It has been assumed that, on vacuum annealed crystals, adsorption of oxygen takes place almost exclusively at bridging oxygen vacancies.[9,10,14−16,21,22] Data in Figure 5 provide evidence to the contrary. The photodesorption portion of the data (hollow squares) was taken by first preparing the crystal as usual with a 10 min anneal at 850 K in a vacuum. Sufficient oxygen to saturate all vacancies (1.8×10^{15} molecules/cm^2) was then dosed at 110 K; the sample was placed in front of the QMS and then exposed to the UV lamp until oxygen evolution ceased. The adsorption/photodesorption cycles were then repeated several times, without any annealing between them. Despite the fact that after the first photodesorption cycle there were no longer any bridging oxygen vacancies (as evidenced by the water TPD in Figure 3c and indirectly by the SSIMS data of Figure 4), a significant amount of oxygen still evolved during the photodesorption portion of the subsequent adsorption/photodesorption cycles. This is in stark contrast to thermal reactions of oxygen upon TiO_2(110): after a single adsorption/TPD cycle, no detectable amount of O_2 was found in the 410 K TPD state in subsequent experiments. Only an anneal at 850 K was able to restore the surface such that the 410 K oxygen TPD state could be observed after O_2 exposure. It appears that the initial photodesorption peak is comprised of two contributions, one from O_2 adsorbed in association with vacancy sites that are deactivated by a single oxygen exposure, and another that is accessible irrespective of the status of the bridging oxygen vacancies. This is consistent with previous observations that at low temperatures oxygen exists on TiO_2(110) in at least two different forms which have different photodesorption cross sections.[14,15] This is also consistent with Brinkley and Engel's observations that propanol can be photooxidized on a surface without bridging oxygen vacancies.[16] A puzzle still to be resolved stems from TPD experiments in which oxygen was dosed on the crystal that had just undergone an adsorption/photodesorption cycle. Under these conditions an 410 K oxygen TPD state is not observed despite the fact that there must be at the start of the temperature ramp adsorbed oxygen on the surface. It is possible that the broad hump observed in O_2 TPD from 100 to 350 K (see Figure 1) originates (at least in part) from the same oxygen that photodesorbs in cycles 2−7 of Figure 5. Other workers have attributed this TPD feature to oxygen adsorbed at step and kink defects,[16] and in fact in experiments performed on powder samples[17] this low-temperature oxygen TPD feature is much larger (relative to the 410 K TPD state) than on single-crystal samples that have been smoothed by repeated vacuum annealing.[9,10] In contrast, we have shown that the signal in this region is considerably larger relative to the 410 K TPD peak when dosing by backfilling as opposed to using a directional doser, suggesting that much of the signal between 100 and 350 K originates from the sample holder.[9] Finally, it should be noted that the thermal and photon driven desorption processes could have different angular distributions, and that this is a possible source of the difference between the measured amounts of oxygen evolved in the two processes. Thus, direct quantitative comparisons between the amounts of thermal and photodesorbed oxygen from oxygen precovered TiO_2(110) will require further work exploring the nonthermal angular distributions typical of photoprocesses.

B. Interactions of Water with Preadsorbed O_2. The amount of oxygen recovered from the 410 K molecular oxygen TPD state is sensitive to the amount of postadsorbed water. Figure 6 is the O_2 TPD peak area data collected from a series of experiments in which the TiO_2(110) sample was first annealed in a vacuum for 10 min, cooled to 115 K, exposed to 3.8×10^{15} molecules/cm^2 O_2 to obtain a sizable 410 K oxygen TPD state, and then exposed to varying amounts of water. The area of the 410 K molecular oxygen TPD state decreased as a function of water exposure. By extrapolating the least-squares line (fit to the first five data points) to zero oxygen signal it, can be seen that the amount of water needed to completely attenuate the 410 K molecular oxygen state is roughly equal to one water monolayer. The difference between the ideal linear behavior and the last few data at high water coverage is due to angular profile differences between water and oxygen emerging from our pinhole aperture doser. The end of the doser is an open stainless steel tube of 0.19 in. i.d., and the length from the pinhole is about 11 in. This arrangement produces well-

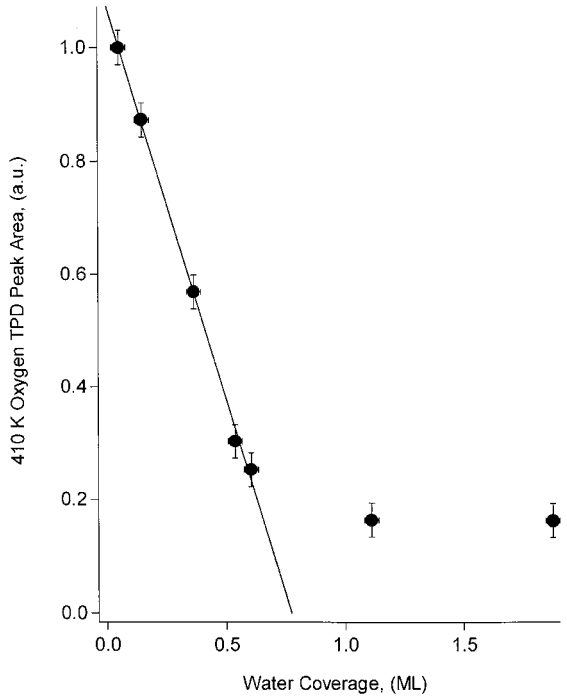

Figure 6. Depletion of the 410 K molecular oxygen state by water. The filled circles represent integrated O_2 TPD data obtained by dosing the vacuum annealed crystal first with O_2 and then with the indicated coverages of water while the crystal was maintained at 115 K.

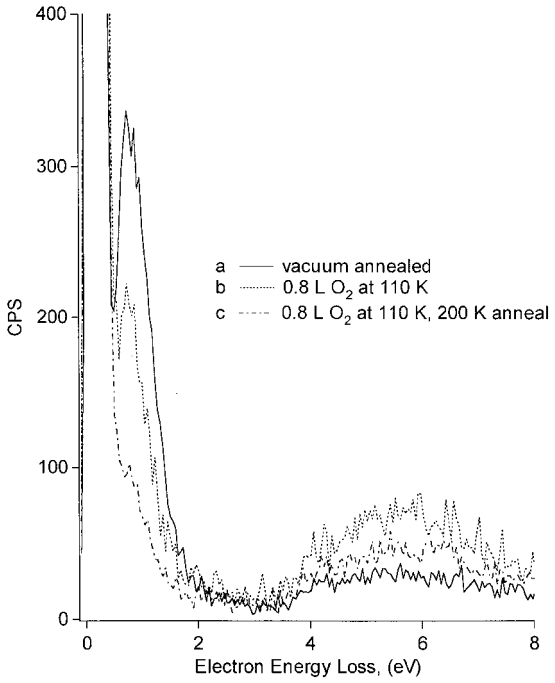

Figure 7. EELS data from the vacuum annealed TiO_2(110) surface, the vacuum annealed surface exposed to 0.8 langmuir of O_2 at 110 K, and the same surface warmed to 200 K. The large loss feature at ~0.8 eV in (a) and (b) is characteristic of Ti^{3+} cations at oxygen vacancies, and the broad feature starting at ~4 eV results from TiO_2 band to band transitions.

collimated beams for "condensable" molecules, those that readily stick to stainless steel at room temperature (i.e., H_2O). In contrast, for noncondensables such as O_2, molecular beams from this doser have a significant angular divergence as they exit the tube. The net result is that during our O_2/water experiments we are dealing with exposure areas that are concentric but are not the same size, with a larger area of the crystal being exposed to O_2 than to H_2O. Thus O_2 molecules comprising the area between the fringes of the water and oxygen spots continue to contribute to the 410 K TPD peak area even after several layers of water are deposited. At high water doses this causes a nonlinear relationship between the depletion of the molecular oxygen TPD state and the total water exposure.

How is it that the monolayer state of water with a TPD maximum below room temperature can attenuate the 410 K molecular oxygen state which desorbs at a significantly higher temperature? Our previous measurements of sticking coefficients of oxygen on TiO_2(110) as well as TPD experiments with coadsorbed $^{16}O_2$ and $^{18}O_2$ indicated that, at low temperatures (115 K), all adsorbed O_2 resides in the shallow potential well of a precursor state.[9] Electron energy loss spectroscopy (EELS) measurements of the vacuum annealed TiO_2(110) surface (Figure 7a) exposed at low temperatures to 0.8 langmuir O_2 (2.8×10^{14} molecules/cm^2) still show the 0.8 eV loss associated with band gap states characteristic of Ti^{3+} cations at oxygen vacancies (Figure 7b). In contrast, warming the same oxygen-dosed surface to 200 K results in almost total attenuation of the peak at 0.8 eV (Figure 7c). It should be noted that the weak, broad loss feature previously observed[9] at 2.8 eV for surfaces with much larger oxygen exposure (20 langmuirs) is not seen here because of its weak oscillator strength.

From the previous arguments one might therefore propose that at 115 K water is able to displace oxygen directly into the gas phase from its physisorbed precursor state. However, experiments in which the oxygen-dosed surface was placed in front of the mass spectrometer and then dosed with a beam of water showed that in fact there was no such displacement occurring (data not shown). The only other possible explanation for the decrease in the amount of oxygen desorbed from the 410 K TPD state with increasing water coverage must involve the oxygen staying on the surface as the product of a chemical reaction. Dujardin et al. observed via UPS and STM a reaction between $O_{2(ad)}$ and H_2O, but did not speculate on the reaction product.[23] Peroxy anions (O_2^{2-}) were predicted as a product of reactions between oxygen vacancies on MgO and water.[24] Hydroperoxy radicals have been proposed as in intermediate in TiO_2 photooxidation reactions.[2,25−27] Yamaguchi et al. performed DFT calculations for the structure of O_2 adsorbed end-on (referred to as η_1-O_2 in a previous publication[9]) on the rutile polymorph of SnO_2(110) and found the O_2 molecule to be in the form of superoxo (O_2) anion.[28] Thus the presence of a hydroperoxy species, which would result from the protonation of O_2^- (reaction 8) formed upon reaction between O_2 and Ti^{3+} cations at O vacancy sites, seems likely, and explains the data in Figure 6 as well as the photolysis experiments discussed below.

C. Postirradiation TPD of Coadsorbed Oxygen and Water. In this section, we discuss results of experiments in which ice overlayers were used in an effort to trap photodesorbing O_2 molecules at the TiO_2(110)−water interface. Figure 8 is a series of postirradiation TPD spectra of $^{18}O_2$ from TiO_2-(110) prepared with varying ice overlayers. For each TPD experiment, the surface was first annealed in the usual manner, cooled to 115 K, dosed with saturation $^{18}O_2$, dosed with water, and finally exposed to 2.1×10^{17} photons/cm^2 ($h\nu = 4.13$ eV). The water exposure was varied from 3 to 65 monolayers, where 1 ML is defined in terms of the number of unit cells per square centimeter on TiO_2(110) (5.2×10^{14}). There were no new oxygen TPD states observed for water coverages below about

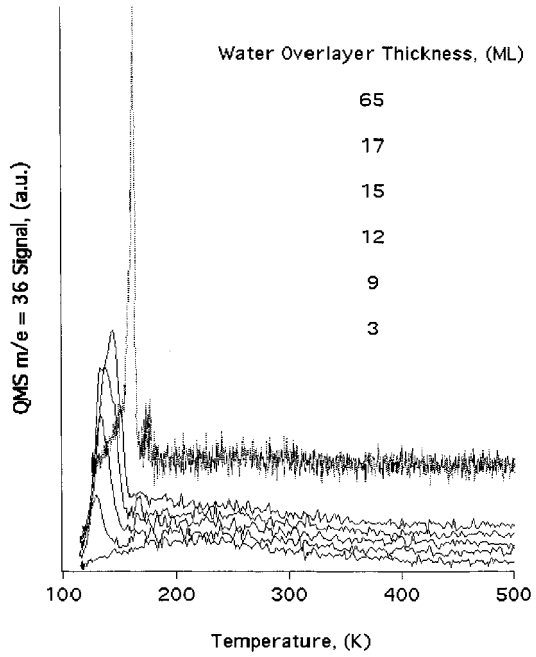

Figure 8. Dependence of the amount of oxygen recovered from the low-temperature O_2 TPD state on the water overlayer thickness.

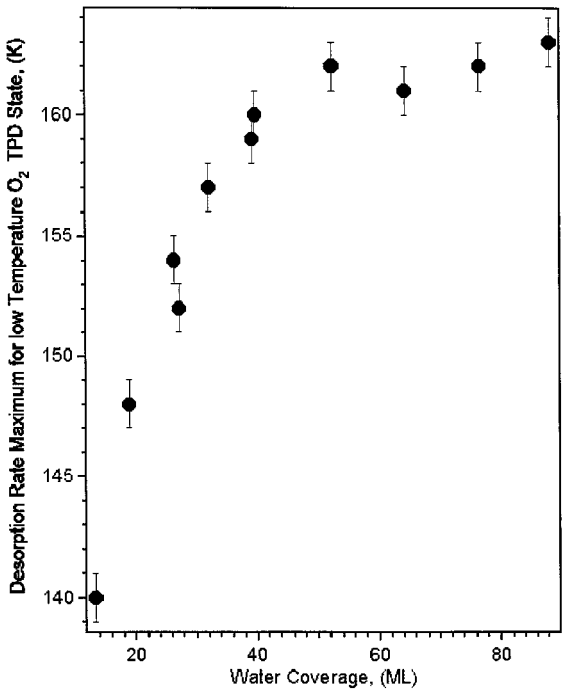

Figure 9. Dependence of the desorption rate maxima of the low-temperature O_2 TPD state on the water overlayer thickness.

10 ML; however for thicker water−ice layers we noted an unusual and previously unobserved oxygen TPD state around 160 K.

The position and full width half-maxima of the O_2 TPD peaks were dependent on the thickness of the water overlayer, with the desorption rate maxima shifting to higher temperature (Figure 9) and sharpening (Figure 8) with increased ice overlayer thickness. For very thick water films the low-temperature O_2 TPD state was extremely sharp, and was found around 160 K. This temperature coincides with the amorphous to crystalline phase transition of water, and as previous workers have found,[29] weakly bound adsorbates under films of amorphous solid water (ASW) have been shown to percolate through cracks in thick ices that develop during this crystallization process. A signature of this "molecular volcano" is a sharp desorption feature at the transition temperature for adsorbates trapped under water films of ~30 ML.[29] (It should be noted that our monolayer definition is in terms of the structure of TiO_2(110), and our water film thicknesses should be divided by a factor of 2 in order to be compared to data in ref 29.) A plot of the O_2 TPD peak maxima versus water film thickness shows that the upward shift in the peak temperature ceases after about 40 ML of H_2O, plateauing at ~160 K. Thus the water film thickness, desorption temperature, and general sharp shape of the TPD state all agree reasonably well with the characteristics of the dynamic percolation model.[29] We were not, however, able to resolve the phase transition point from the ice desorption peak, which Smith et al.[29] accomplished by employing a 0.6 K/s ramp, a factor of 3 slower than used in this study. Alternatively, since the maximum peak temperature for the O_2 state ends up at exactly the same point as the ice peak temperature, it is also possible that O_2 desorbs not at the phase transition, but as the ice itself is desorbed. A release process dependent on diffusion of the oxygen through the water film cannot be ruled out since the temperature of the desorption maxima shifts upward as a function of the ice film thickness.

The data in Figures 8 and 9 therefore indicate that photocatalytically produced O_2 can be trapped at the TiO_2(110) interface with a sufficiently thick ice layer and that these O_2 molecules do not return to their previous chemical state after being trapped at the interface.

Now remains the task of identifying the source of the photopromoted oxygen. This issue is partially resolved by the fact that the observed molecules being desorbed were isotopically identical with those dosed on the crystal (i.e., $^{18}O_2$), indicating that no oxygen−surface or oxygen−water exchange processes have taken place. Additionally, from the previously discussed experiments it is known that oxygen is present on the surface in some form. Since the available information indicates our low-temperature oxygen TPD state results from a chemical species created from diatomic oxygen and water, and is one in which the O−O bond is preserved, a likely candidate for the photocatalytically active species is $H_2O_{2(ad)}$ or HO_2^-. Alternatively, the photoactivation process could result in a triplet-to-singlet conversion in O_2 with the singlet state being bound more weakly at the vacancy than the triplet state. Small diamagnetic molecules such as CO,[30] CO_2,[31] and N_2[32] interact weakly with vacancy sites, whereas paramagnetic molecules such as (triplet) O_2[9] and NO[33] bind strongly and exhibit robust chemistry. However, at this point we have no evidence for a triplet-to-singlet transition in O_2, and we favor an H_2O_2 or HO_2^- species based on the water + O_2 TPD results.

Since formation of the peroxy species should be complete well before the 3 ML thickness of the bottommost trace of Figure 8, one might wonder why a TPD state is not seen at low water coverages. When the O_2/TiO_2(110) system is capped with thin water films and then exposed to UV, what is observed in isothermal photodesorption experiments conducted at 115 K is an immediate strong oxygen pulse from the crystal's surface. It is possible that an explanation for this behavior is provided by recent work showing that amorphous solid water films can undergo crystallization when exposed to UV irradiation.[34] In this work, the authors show that photocrystallization occurs primarily in the first few monolayers of a water film. Thus we believe that for our experiments with thin water films we are simultaneously photochemically generating oxygen and providing a means for it to escape (percolation through photocrystal-

lized ice), whereas for thicker water films the crystallization and oxygen release occur thermally during H_2O desorption.

IV. Conclusions

In trying to simulate the TiO_2−solution interface, we have learned that oxygen adsorbed on TiO_2(110) at 115 K is not completely removed by prolonged exposure to 4.1 eV radiation, an important result that helps explain why high photodesorption cross sections do not prevent photooxidation reactions from occurring. We have found evidence for the production of a photocatalytically active chemical intermediate, tentatively identified to be a hydrogen peroxy species, that is formed at 115 K on TiO_2(110) in a reaction involving coadsorbed oxygen and water. This chemical intermediate can be photolyzed by band gap irradiation, with the production of molecular oxygen. This photoproduced O_2, which may be more chemically active than ground-state O_2, does not return to its previous chemical state but is trapped transiently at the TiO_2−water interface if the water overlayers are thick enough to resist photocrystallization. Since the concentration of organic molecules in TiO_2-based photooxidation reactions should be at a local maximum at the TiO_2−solution interface, the behavior of the oxygen species studied here is relevant to understanding these complex heterogeneous reactions.

Acknowledgment. This work was supported by the U.S. Department of Energy, Office of Basic Energy Sciences, Division of Materials Sciences, and the Environmental Management Science Program. Pacific Northwest National Laboratory is a multiprogram national laboratory operated for the U.S. Department of Energy by Battelle Memorial Institute under Contract No. DE-AC06-76RLO 1830. The research reported here was performed in the William R. Wiley Environmental Molecular Science Laboratory, a Department of Energy user facility funded by the Office of Biological and Environmental Research.

References and Notes

(1) Linsebigler, A. L.; Lu, G.; Yates, J. T., Jr. *Chem. Rev.* **1995**, *95*, 735.
(2) Heller, A. *Acc. Chem. Res.* **1995**, *28*, 503.
(3) Vidal, R. A.; Bahr, D.; Baragiola, R. A.; Peters, M. *Science* **1997**, *276*, 1839.
(4) Grün, E.; Baguhl, M.; Hamilton, D. P.; Riemann, R.; Zook, H. A.; Dermott, S.; Fechtig, H.; Gustafason, B. A.; Hanner, M. S.; Horányi, M.; Khurana, K. K.; Kissel, J.; Kivelson, M.; Lindblad, B. A.; Likert, D.; Likert, G.; Mann, I.; McDonnell, J. A. M.; Morfill, G. E.; Polanskey, C.; Schwehm, G.; Srama, R. *Nature* **1996**, *381*, 395.
(5) Turner, B. E. *Astrophys. J.* **1996**, *468*, 694.
(6) Muggli, D. S.; Falconer, J. L. *J. Catal.* **1999**, *181*, 155.
(7) Lu, G.; Linsebigler, A.; Yates, J. T., Jr. *J. Phys. Chem.* **1995**, *99*, 7626.
(8) Tatsuma, T.; Tachibana, S.; Miwa, T.; Tryk, D. A.; Fujishima, A. *J. Phys. Chem. B* **1999**, *103*, 8033.
(9) Henderson, M. A.; Epling, W. S.; Perkins, C. L.; Peden, C. H. F.; Diebold, U. *J. Phys. Chem. B* **1999**, *103*, 5328.
(10) Epling, W. S.; Peden, C. H. F.; Henderson, M. A.; Diebold, U. *Surf. Sci.* **1998**, *412/413*, 333.
(11) Henderson, M. A. *Surf. Sci.* **1994**, *319*, 315. Henderson, M. A. *Langmuir* **1996**, *12*, 5093.
(12) Hugenschmidt, M. G.; Gamble, L.; Campbell, C. T. *Surf. Sci.* **1994**, *302*, 329.
(13) Brinkley, D.; Dietrich, M.; Engel, T.; Farrall, P.; Gantner, G.; Schafer, A.; Szuchmacher, A. *Surf. Sci.* **1998**, *395*, 292.
(14) Lu, G.; Linsebigler, A.; Yates, J. T., Jr. *J. Chem. Phys.* **1995**, *102*, 4657.
(15) Rusu, C. N.; Yates, J. T., Jr. *Langmuir* **1997**, *13*, 4311.
(16) Brinkley, D.; Engel, T. *Surf. Sci.* **1998**, *415*, L1001.
(17) Yanagisawa, Y.; Ota, Y. *Surf. Sci.* **1991**, *254*, L433.
(18) Henrich, V. E.; Cox, P. A. *The Surface Science of Metal Oxides*; Cambridge University Press: Cambridge, 1996; p 118.
(19) Furube, A.; Asahi, T.; Masuhara, H.; Yamashita, H.; Anpo, M. *J. Phys. Chem. B* **1999**, *103*, 3120.
(20) Kasinski, J. J.; Gomez-Jahn, L. A.; Faran, K. J.; Gracewski, S. M.; Dwane Miller, R. J. *J. Chem. Phys.* **1989**, *90*, 1253.
(21) Pan, J. M.; Maschhoff, B. L.; Diebold, U.; Madey, T. E. *J. Vac. Sci. Technol., A* **1992**, *10*, 2470.
(22) Lu, G.; Linsebigler, A.; Yates, J. T., Jr. *J. Phys. Chem.* **1994**, *98*, 11733.
(23) Dujardin, G.; Mayne, A.; Comtet, G.; Hellnre, L.; Jamet, M.; Le Goff, E.; Millet, P. *Phys. Rev. Lett.* **1996**, *76*, 3782.
(24) King, B. V.; Freund, F. *Phys. Rev. B* **1984**, *29* (10), 5814−5824.
(25) Meriaudeau, P.; Vedrine, J. C. *J. Chem. Soc., Faraday Trans.* **1976**, *72*, 472.
(26) Gonzalez-Elipe, A. R.; Munuera, G.; Soria, J. *J. Chem. Soc., Faraday Trans.* **1979**, *75*, 748.
(27) Bahnemann, D. W.; Hilgendorff, M.; Memming, R. *J. Phys. Chem. B* **1997**, *101*, 4265−4275.
(28) Yamaguchi, Y.; Nagasawa, Y.; Shimomura, S.; Tabata, K.; Suzuki, E. *Chem. Phys. Lett.* **2000**, *316*, 477.
(29) Smith, R. S.; Huang, C.; Wong, E. K. L.; Kay, B. D. *Phys. Rev. Lett.* **1997**, *79*, 909.
(30) Linsebigler, A.; Lu, G.; Yates, J. T., Jr. *J. Chem. Phys.* **1995,** *103*, 9438.
(31) Henderson, M. A. *Surf. Sci.* **1998**, *400*, 203.
(32) Rittner, F.; Fink, R.; Boddenberg, B.; Staemmler, V. *Phys. Rev. B* **1998**, *57*, 4160.
(33) Sorescu, D. C.; Rusu, C. N.; Yates, J. T., Jr. *J. Phys. Chem. B* **2000**, *104*, 4408.
(34) Chakarov, D.; Kasemo, B. *Phys. Rev. Lett.* **1998**, *81* (23), 5181−5184.